

Self-assembled magnetic nitride dots on Cu(100) surfaces

J. M. Gallego,¹ S. Yu Grachev,² M. C. G. Passeggi, Jr.,³ F. Sacharowitz,⁴ D. Ecija,⁵ R. Miranda,⁵ and D. O. Boerma⁵

¹*Instituto de Ciencia de Materiales de Madrid, CSIC, Cantoblanco, 28049 Madrid, Spain*

²*NVSV, Materials Science Centre, University of Groningen, Nijenborgh 4, 9737 AG, The Netherlands*

³*Instituto de Desarrollo Tecnológico para la Industria Química-INTEC, Güemes 3450, 3000-Santa Fe, Argentina*

⁴*Freie Universität Berlin, Fachbereich Physik, Arnimallee 14, 14195 Berlin, Germany*

⁵*Departamento de Física de la Materia Condensada, Universidad Autónoma de Madrid, Cantoblanco, 28049 Madrid, Spain*

(Received 1 October 2003; revised manuscript received 13 January 2004; published 12 March 2004)

We describe here a procedure for the *direct* fabrication of a self-organized, ordered pattern of Fe₄N magnetic dots on an otherwise clean Cu(100) surface. It is based on the evaporation of Fe in a flux of atomic N produced by a plasma source onto a Cu(100) surface kept at 700 K. The large-scale morphology of the surface is demonstrated by scanning tunneling microscope. The average lateral size of the islands is 10 nm and they penetrate three to four layers into the substrate. The iron nitride dots present a characteristic $p4g(2\times 2)$ surface reconstruction, detected also on 25 nm thick, nonstructured films grown in the same conditions, on which x-ray diffraction, conversion electron Mössbauer spectroscopy, Rutherford backscattering spectroscopy, and magneto-optic Kerr effect confirm the existence of a pure magnetic, cubic, γ' -Fe₄N(100) layer epitaxial with the Cu(100) substrate.

DOI: 10.1103/PhysRevB.69.121404

PACS number(s): 68.37.Ef, 68.65.Hb, 81.16.Dn

The controlled fabrication of magnetic nanostructures is important for future advances in magnetic recording media, tunnel junctions, and magnetic-random access memories. There are two main avenues widely explored at present: sub-micron *e*-beam lithography of magnetic films¹ and self-organized growth² on nanostructured surfaces which act as template for the directed growth of the magnetic material. The first surface features used to grow monolayer or bilayer-high stripes or nanowires were the steps of vicinal surfaces.^{2,3} Laterally ordered, self-organized, *nanodots* of Co, Ni, or Fe with a density of $4 \times 10^{12} \text{ cm}^{-2}$ have been grown on reconstructed surfaces, such as Au(111),^{4,5} taking advantage of the preferential nucleation that occurs at the corners of the herringbone reconstruction. The dots, however, due to their limited vertical size do not contain enough magnetic material and are superparamagnetic above 30 K. Perpendicularly magnetized Co *pillars* have also been produced on Au(111) by alternate evaporation of Co and Au.⁶

More recently, “nanoengineered” surfaces were fabricated to be used as templates for the growth of magnetic nanostructures. Among these we may cite the self-organized, two-dimensional (2D) periodic arrays of SiGe pyramids on Si(100) surfaces⁷ and the N implanted Cu(100) surfaces.⁸ In this latter system, a Cu(100) crystal was bombarded with a preselected dose of N⁺ ions and annealed to 600 K, which gives rise to an ordered array of square $c(2\times 2)$ islands containing N, which separate a grid of narrow Cu lines.⁹ Co nanolines,^{10,11} 1 ML (monolayer) high, have been observed to grow on top of the Cu lines forming the grid. Ni (Ref. 12) and Fe,^{13–15} on the other hand, form dots at the intersections of the Cu grid. The density of dots is again $4 \times 10^{12} \text{ cm}^{-2}$. They do not contain enough material to be ferromagnetic at 300 K. Furthermore, two steps are required for the formation of the nanostructured magnetic film (N modification of the substrate plus magnetic metal deposition) and the magnetic materials grow *on* the clean Cu patches of the surface. This jeopardizes its possible use at temperatures above 300 K,

since it has been amply documented¹⁶ that the poorly controlled interdiffusion processes between Cu and the cited magnetic metals affect their magnetic properties.

We describe here a procedure to grow nanostructured layers of a magnetic material, namely the γ' cubic iron nitride (Fe₄N) on Cu(100) surfaces using a single step in the fabrication process and reducing considerably the intermixing between Fe and Cu. Recently iron nitrides are attracting interest because of their exciting magnetic properties.¹⁷ In particular, the growth of nanostructured epitaxial films of Fe₄N is relevant in the context of the proposed fabrication of all-nitride, submicron, magnetic tunnel junctions.¹⁸

The experiments were performed in an ultrahigh vacuum (UHV) chamber (base pressure = 2×10^{-10} mbar) equipped with a home-made scanning tunneling microscope (STM) and a rear view low-energy electron-diffraction (LEED) optics also used for Auger electron spectroscopy (AES). The main chamber was connected to an independently pumped, home-built radio-frequency (rf) plasma discharge source.¹⁹ The Cu(100) substrate was cleaned by cycles of sputtering and annealing at 900 K. Iron was evaporated using an electron gun and, in order to obtain ordered arrays of iron nitride islands (see below), unusually slow deposition rates in the range of 0.05 ML/min were used. In order to grow Fe-N films, during the deposition of Fe the sample was simultaneously exposed to a flux of atomic N (actually a mixture of N and H) coming from the rf source. The presence of H₂ in the gas promotes the growth of the pure Fe₄N phase.^{19,20} The substrate was kept at 700 K during the growth of the Fe-N layers. This method was used before to grow single-crystal, epitaxial films of γ' -Fe₄N on MgO(100) (Ref. 21) and Cu(100) substrates.²² The vacuum in the UHV chamber was in the 10^{-7} – 10^{-8} mbar range during deposition. All measurements reported here (STM, AES, LEED) were performed after cooling the sample to 300 K.

Exposure of the Cu(100) surface at 700 K to a total dose of 2.3 ML of Fe evaporated at a slow deposition rate in the

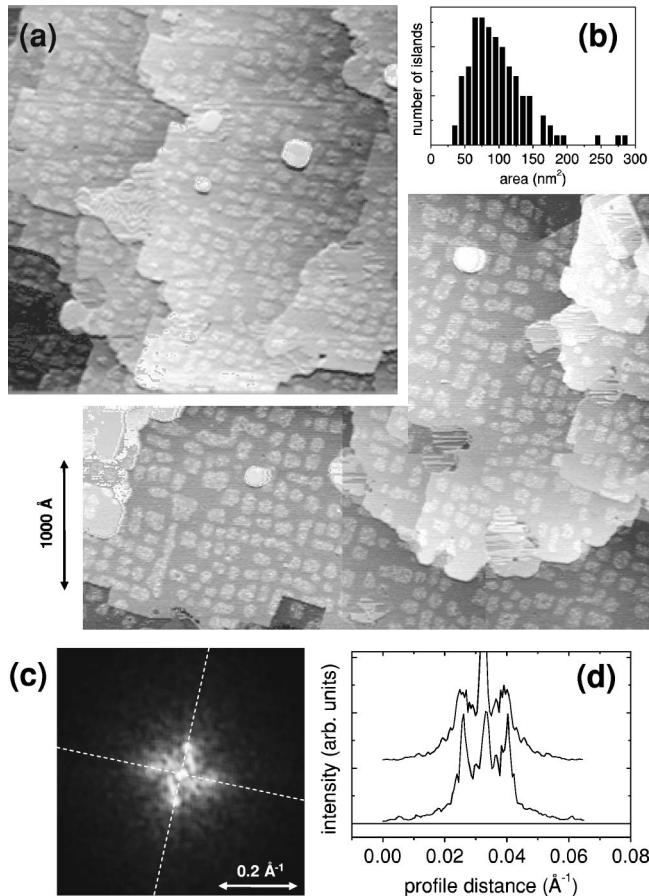


FIG. 1. (a) Representative composition of large-scale STM images (covering $0.5 \mu\text{m}$, see the bar corresponding to 1000 \AA) recorded on different spots of the surface of a Cu(100) crystal exposed during 50 min at 700 K to a flux of Fe+N. The total dose was 2.3 ML of Fe and a 1×10^{-2} mbar of a 1:1 mixture of N_2 and H_2 was employed in the rf source; (b) size distribution of the nitride islands; (c) Fourier transform of the STM images [taken from the lower left of (a)]; (d) intensity profiles along the two lines drawn in (c). The separation between peaks corresponds to an average distance between islands of 14 nm.

presence of a beam of atomic nitrogen results in a surface whose large-scale morphology is shown in the STM images of Fig. 1. The surface is covered with islands of square or rectangular shape with their edges aligned along $\langle 001 \rangle$ directions. Their average height is $\sim 0.8 \text{ \AA}$ above the substrate. The island size distribution is shown in Fig. 1(b). The average lateral size is 10 nm. The islands are spatially self-organized, in the sense that they display an additional long-range organization which results in a rather ordered 2D array. The degree of long-range order is remarkable for a single-step growth process, as shown by the Fourier transform of the STM images [see Fig. 1(c)]. Figure 1(d) shows the existence of well-defined side peaks in the line profiles of the Fourier transform. This indicates that there is a preferential distance between the islands. The separation of the side peaks with respect to the central one translates into an average distance between islands of 14 nm. This corresponds to an island density of $5.1 \times 10^{11} \text{ cm}^{-2}$.

A blowup of the islands appears in the left part of Fig. 2.

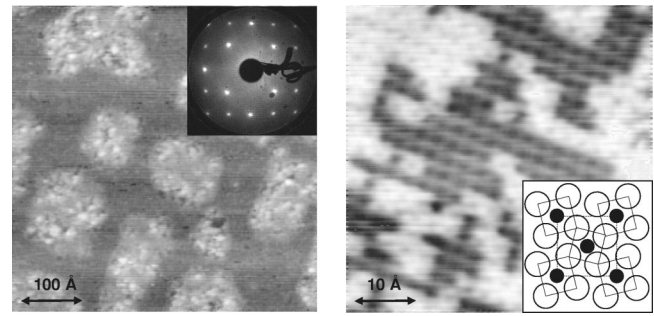


FIG. 2. The left panel shows a zoom into the surface of the Cu(100) crystal exposed to Fe and N at 700 K displayed in Fig. 1. The inset reproduces the $p4g(2 \times 2)$ LEED pattern corresponding to this surface ($E_p = 110 \text{ eV}$). The right panel reproduces a higher magnification image (recorded on a different surface) showing the atomic arrangement of the $p4g(2 \times 2)$ reconstruction. The inset shows schematically the proposed atomic model of the $p4g(2 \times 2)$ reconstruction (full circles, N atoms; empty circles, Fe atoms).

The surface of the islands shows apparent inhomogeneities, while the surface between the islands is homogeneous. Figure 3(a) shows the AES spectrum recorded at the sample of Fig. 1. The presence of both Fe and N at the surface is clearly demonstrated. Since the surface surrounding the islands does not show any sign of Fe or N inclusions (easily detected by STM) and increasing the exposure increases the density of islands, we assign the patches in between the islands to clean Cu and the islands to a compound of Fe and N. The Fe-N islands must then *penetrate several (three to four) layers into the substrate* for the intensity ratio of the Fe and Cu peaks to be consistent with the morphology revealed by STM.²³

The inset in the left panel of Fig. 2 reproduces the LEED pattern observed on the surface of Fig. 1 that shows a $p4g(2 \times 2)$ superstructure characterized by the absence of the four first half-order spots of the simple 2×2 pattern. The STM image of the right panel of Fig. 2 shows the weaving pattern of the atomic arrangement at the surface of a similar Fe-N film. Low-energy ion scattering measurements and first-principles calculations indicate that the surface reconstruction consists of N atoms, imaged as depressions, sitting on fourfold hollow sites of a twisted square array of Fe at

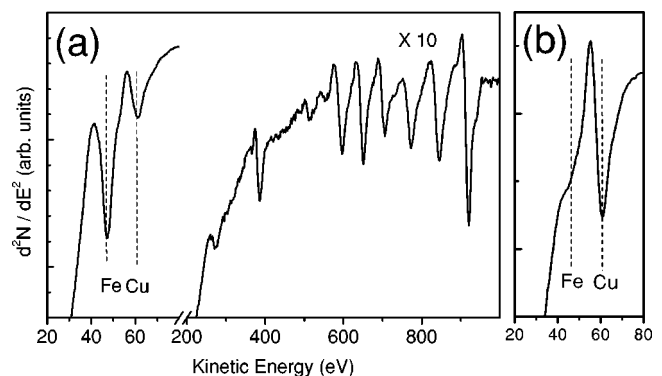


FIG. 3. AES spectra corresponding to (a) 2.3 ML of Fe evaporated on Cu(100) in the flux of N at 700 K, and (b) 1.3 ML of pure Fe evaporated on Cu(100) at 700 K.

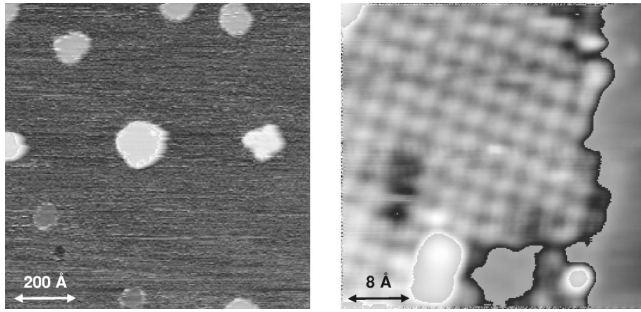


FIG. 4. Large-scale STM image recorded on a Cu(100) surface exposed to 0.3 ML of pure Fe at 700 K. The atomically resolved image at the right shows the $c(2 \times 2)$ superstructure observed on top of the Cu islands (see text).

oms 2.6 Å apart.²⁴ The proposed surface arrangement, schematically shown in the inset of the right panel, is similar to the one originating the $p4g(2 \times 2)$ “clock” reconstruction of N or C on Ni(100).^{25,26}

In order to identify the composition and crystalline structure of the Fe-N phase forming the islands, we have deposited Fe in the presence of N in similar conditions until films thick enough to allow for x-ray diffraction, conversion emission Mössbauer spectroscopy, magneto-optic Kerr effect, low-energy ion scattering, or Rutherford backscattering analysis were produced. These data (to be described in detail elsewhere²⁷) allow us to identify the islands as γ' -Fe₄N, (100)-oriented. In γ' -Fe₄N the iron atoms form a fcc sublattice ($a_{\gamma'} = 3.795$ Å, while $a_{\text{Cu}} = 3.615$ Å), with the N atom in the center of the cube. Thus, the crystalline structure contains alternating planes of pure Fe and Fe/N along the (100) direction. In the latter, the N atoms are located in the center of Fe squares. These planes of the bulk nitride are closely related to the $p4g(2 \times 2)$ surface reconstruction.²⁴ Even for 200 ML thick Fe₄N(100) films, the $p4g(2 \times 2)$ LEED pattern and the STM atomically resolved surface structure are identical to those observed on the self-organized islands reported here.

The high temperature of the growth of the iron nitride was chosen in order to produce a single phase, crystalline and epitaxial (at lower temperatures other phases, such as ϵ -Fe₃N, are also present and the iron nitride films are nanocrystalline). One has to wonder, however, why the elevated growth temperature does *not* produce strong interdiffusion of Fe and Cu. It is well known that the Fe-on-Cu system is metastable, i.e., the surface free energy of Fe (2.9 J m^{-2}) is significantly greater than the surface energy of Cu (1.9 J m^{-2}) so Cu has a strong tendency to segregate to the surface.^{28,29} In fact, depositing *pure* Fe on Cu(100) surface at 700 K *does result* in interdiffusion. The STM image at the left of Fig. 4 shows the initial stages of the deposition (0.3 ML) of Fe on Cu(100) at 700 K, with no N present. There are islands of irregular shape with a density $7 \times 10^{10} \text{ cm}^{-2}$ and an average lateral size of 10 nm. The surface of the islands is atomically flat and atomic resolution STM images (Fig. 4, right) show a square array of atomic protrusions separated 3.6 Å, i.e., forming a $c(2 \times 2)$ arrangement with respect to the underlying Cu(100) substrate. The LEED pat-

tern at low energies also displays the $c(2 \times 2)$ symmetry. Fe is not detected by AES in these conditions. The AES spectrum shown in Fig. 3(b) demonstrates that even after deposition of 1.3 ML of Fe at 700 K the signal corresponding to Fe is barely discernible. We assume, thus, that the surface of the islands is composed exclusively of Cu atoms extracted from the substrate. The islands probably nucleate on top of buried Fe patches. Similar observations at higher Fe coverages²⁷ indicate that without the presence of the beam of atomic N, the Fe films grown at 700 K would be buried by a thick Cu layer.

Why do the Fe-N islands form and why do they self-organize? At this stage we may only speculate that the growth of the nitride film may start, just as in the case of pure Fe (since the segregation energy is positive),³⁰ with the fast exchange of the deposited Fe atoms with the Cu atoms from the substrate.³¹ It is known that the surface mobility of Cu on Cu(100) is very high at 700 K. The Cu atoms ejected from the substrate, then, almost certainly diffuse to the existing steps. Now, since the two metals do not mix,^{30,32} the Fe atoms will tend to agglomerate into clusters at the surface. At the same time (since the N-Fe bond is stronger than the N-Cu bond), the N atoms would react preferentially with the Fe atoms to form the iron nitride. On the basis of calculations that indicate a substantially lower energy for the N terminated surface of γ' -Fe₄N with respect to the Fe terminated surface,²⁴ we suggest that the adsorption of N on the Fe patches causes a decrease of the surface free energy of the islands large enough to prevent the segregation of the Cu atoms to the surface of the islands.

Pattern formation in self-organized systems is often the result of a competition of short-range, attractive interactions and long-range, repulsive interactions. In our case, we suggest that the long-range forces deriving from the difference of surface stress between the Fe₄N islands and the clean Cu patches are responsible for the self-organization, i.e., the additional long-range order of the Fe₄N islands shown in Fig. 1. The self-organization of the nitride islands into an ordered square array described here resembles closely the 2D square grid pattern found on the Cu(001)- $c(2 \times 2)$ N surface.⁸ In that case, the surface stress changes from tensile to compressive for the bare and nitrogen-covered surface regions, respectively. The formation of this and other self-organized patterns, such as the stripe phase of Cu(110)-(2 × 1)O (Ref. 33) or the regularly spaced vacancy islands formed on Cu(100) upon bombarding,³⁴ has been attributed to the minimization of the elastic energy due to surface stress spatial variations.^{35,36} A similar mechanism might be operating in this system. In any case, the process of minimization of the total surface stress involves in our case slow, long-range transport of matter as indicated by the fact that very low Fe deposition rates are required for the islands to self-organize. In fact, the Fe₄N islands are laterally disordered if the evaporation of Fe is carried out at the “standard” deposition rate of 0.5 ML/min.

This work was supported by the Spanish CICyT (under Grant No. MAT2001-0082-C04-02) and DGI (under Grant No. BFM2001-0174).

- ¹C.A. Ross, S. Haratani, F.J. Castao, Y. Hao, M. Hwang, M. Shima, J.Y. Cheng, B. Vögeli, M. Farhoud, M. Walsh, and H.I. Smith, *J. Appl. Phys.* **91**, 6848 (2002).
- ²J. de la Figuera, M.A. Huerta-Garnica, J.E. Prieto, C. Ocal, and R. Miranda, *Appl. Phys. Lett.* **66**, 1006 (1995).
- ³J. Shen, R. Skomski, M. Klaua, H. Jenniches, S.S. Manoharan, and J. Kirschner, *Phys. Rev. B* **56**, 2340 (1997).
- ⁴D.D. Chambliss, R.J. Wilson, and S. Chiang, *Phys. Rev. Lett.* **66**, 1721 (1991).
- ⁵B. Voigtlander, G. Meyer, and N.M. Amer, *Phys. Rev. B* **44**, 10354 (1991).
- ⁶O. Fruchart, M. Klaua, J. Barthel, and J. Kirschner, *Phys. Rev. Lett.* **83**, 2769 (1999).
- ⁷For a recent review, see Ch. Teichert, *Phys. Rep.* **365**, 335 (2002).
- ⁸F.M. Leibsle, C.F.J. Flipse, and A.W. Robinson, *Phys. Rev. B* **47**, 15865 (1993).
- ⁹T.M. Parker, L.K. Wilson, N.G. Condon, and F.M. Leibsle, *Phys. Rev. B* **56**, 6458 (1997).
- ¹⁰Y. Matsumoto and K. Tanaka, *Jpn. J. Appl. Phys., Part 2* **37**, L154 (1998).
- ¹¹S. D'Adatto, C. Binns, and P. Finetti, *Surf. Sci.* **442**, 74 (1999).
- ¹²K. Mukai, Y. Matsumoto, K. Tanaka, and F. Komori, *Surf. Sci.* **450**, 44 (2000).
- ¹³S.L. Silva, C.R. Jenkins, S.M. York, and F.M. Leibsle, *Appl. Phys. Lett.* **76**, 1128 (2000).
- ¹⁴S. Ohno, K. Nakatsuji, and F. Komori, *Surf. Sci.* **493**, 539 (2001).
- ¹⁵S. Ohno, K. Nakatsuji, and F. Komori, *Surf. Sci.* **523**, 189 (2003).
- ¹⁶See, for instance, J. Shen, Ch.V. Mohan, P. Ohresser, M. Klaua, and J. Kirschner, *Phys. Rev. B* **57**, 13674 (1998), and references therein.
- ¹⁷J.M.D. Coey and P.A.I. Smith, *J. Magn. Magn. Mater.* **200**, 405 (1999).
- ¹⁸D.M. Borsa, S. Grachev, C. Presura, and D.O. Boerma, *Appl. Phys. Lett.* **80**, 1823 (2002).
- ¹⁹S. Yu. Grachev, Ph.D. thesis, University of Groningen, 2003.
- ²⁰S.Yu. Grachev, D.M. Borsa, and D.O. Boerma, *Surf. Sci.* **516**, 159 (2002).
- ²¹D.M. Borsa, S. Grachev, D.O. Boerma, and J.W.J. Kerssemakers, *Appl. Phys. Lett.* **79**, 994 (2001).
- ²²D.O. Boerma, S.Y. Grachev, D.M. Borsa, R. Miranda, and J.M. Gallego, *Surf. Rev. Lett.* **10**, 405 (2003).
- ²³The small amounts of C and O present in Fig. 3(a) appear only after cooling the sample at room temperature, and they might correspond to the small irregular grains visible in Fig. 2 on top of the islands.
- ²⁴F. Yndurain *et al.* (unpublished).
- ²⁵J.H. Onuferko, D.P. Woodruff, and B.W. Holland, *Surf. Sci.* **87**, 357 (1979).
- ²⁶L. Wenzel, D. Arvanitis, W. Daum, H.H. Rotermund, J. Stöhr, K. Baberschke, and H. Ibach, *Phys. Rev. B* **36**, 7689 (1987).
- ²⁷J. M. Gallego *et al.* (unpublished).
- ²⁸Th. Detzel and N. Memmel, *Phys. Rev. B* **49**, 5599 (1994).
- ²⁹J. Shen, J. Giergiel, A.K. Schmid, and J. Kirschner, *Surf. Sci.* **328**, 32 (1995).
- ³⁰A. Christensen, A.V. Ruban, P. Stoltze, K.W. Jacobsen, H.L. Skriver, J.K. Norskov, and F. Besenbacher, *Phys. Rev. B* **56**, 5822 (1997).
- ³¹K.E. Johnson, D.D. Chambliss, R.J. Wilson, and S. Chiang, *J. Vac. Sci. Technol. A* **11**, 1654 (1993).
- ³²D. Spisák and J. Hafner, *Phys. Rev. B* **64**, 205422 (2001).
- ³³K. Kern, H. Niehus, A. Schatz, P. Zeppenfeld, J. George, and G. Comsa, *Phys. Rev. Lett.* **67**, 855 (1991).
- ³⁴M. Ritter, M. Stindtman, M. Farle, and K. Baberschke, *Surf. Sci.* **348**, 243 (1996).
- ³⁵C. Cohen, H. Ellmer, J.M. Guigner, A. L'Hoir, G. Prvot, D. Schmaus, and M. Sotto, *Surf. Sci.* **490**, 336 (2001).
- ³⁶H. Ibach, *Surf. Sci. Rep.* **29**, 193 (1997).